5.8.18

MASTER

BNL--30812

DE82 012722

BNL 30812

MAGNETIC SCANNING OF LWR FUEL ASSEMBLIES

S. Fiarman and A. Moodenbaugh

CONF-8009258--

I. INTRODUCTION

The Agency requires a method to uniquely identify both unirradiated and irradiated LWR fuel assemblies.[1] Although considerable effort has been devoted to this problem in the U.S. and Europe[2], a completely satisfactory solution is still lacking.[3]

Non-destructive assay (NDA) techniques are available both for fresh and spent fuel, but generally are too time consuming and do not uniquely identify an assembly. We report a new method to obtain a signature from a magnetic scan of each assembly. This scan is an NDA technique that detects magnetic inclusions. It is potentially fast (5 min/assembly), and may provide a unique signature from the magnetic properties of each fuel assembly.

Since about 1977, GE's Wilmington fuel fabrication facility has been scanning gadolinium doped rods with a magnetic system called MAPS.[4] On occasion, during the data analysis of rods, spikes were noted in the magnetic system output. These spikes were later identified as ferromagnetic inclusions, probably iron or an iron oxide, that enter the UO_2 powder from iron sieves abrasively worn during processing of the powder. The magnitude and frequency of these inclusions are process dependent but can be controlled by the choice of sieve material and the frequency of sieve replacement. G.E. recognized the potential use of these inclusions in an identification scheme for fuel bundles and applied for a patent.[5] We became aware of this method during a visit to GE, Wilmington in 1978 and since then have actively pursued the development of this concept. Last year, BNL, with the generous assistance of GE, has carried out a modest experimental program to obtain data on our magnetic fuel scanning system and on magnetic properties of UO_2 pellets and small assemblies.

II. EXPERIMENTAL PROGRAM

G.E. Wilmington's fabrication facility lent us 86 UO_2 pellets. Sixty-six pellets contained no or very small magnetic inclusions while 20 contained inclusions. The approximate sizes of the inclusions measured by G.E. were provided with the pellets. Inclusion sizes ranged up to 1-2000 ppm by volume.

A. Magnetization Curves for UO_2 Pellets

The magnetization curves for the first batch of 26 pellets were measured with a vibrating sample magnetometer.[6] Typical magnetization curves for two pellets, one with and one without an inclusion, are shown in Fig. 1. The linear curve of the pellet with no inclusion (a) is typical for paramagnetic substances; magnetization is proportional to the driving field strength, H. The UO_2 has a relatively strong paramagnetic susceptibility of 2360×10^{-6} cgs units.[7] Curve (b) for a pellet with an inclusion resembles the sum of the UO_2 magnetization and the magnetization of a small ferromagnetic particle with a very low coercive force shown in curve (c). The saturation field is about 2 Kilogauss and the ratio of curve (b) to curve (a) is constant between zero and several hundred gauss. This constant ratio will permit a lightweight magnetic scanning system to operate at any convenient modest field with no loss in signal-to-noise.

B. An a.c. Magnetic Scanning System for Pellets

A small mutual inductance scanning system capable of handling a zircaloy rod containing UO_2 pellets was designed and constructed (Fig. 2). An a.c. driving field coil magnetizes the pellets ($\sim$30 gauss at 20 cps) and two bucking coils of equal turns pick up the induced EMF. The combined EMF induced in the pick-up coils was detected by a lock-in amplifier (PAR-124A) whose d.c. output was connected to a chart recorder. A schematic diagram of the system electronics is shown in Fig. 3.

As 5 pellets with no inclusions are lowered at a uniform speed through the coil system, the induced EMF in the bucking coils takes on the characteristic time response shown in Fig. 4. Each pellet with an inclusion sandwiched by 3 pellets with no inclusions on either side was passed through the coil and a qualitative value of the size of the inclusion was measured (see Fig. 5). Since geometric factors such as the shape and orientation of the inclusion and the radial position of the inclusion in the pellet strongly influence the magnetization and the coils' response, the magnitude of the output signal on the chart recorder is not strictly comparable to other type measurements. However, qualitative agreement with G.E.'s inclusion size measurements were obtained.

The 6 pellets with no inclusions that sandwiched the pellet with the inclusion in the above measurements moved the UO_2 "end-effect" away from the inclusion effect (see Fig. 5). In a real fuel rod the UO_2 end-effects would only influence the response of the last few inches of a 14' rod. However, the density variation of the pellets (approximately 3-5%) would produce a random background UO_2 signal. The inclusion-to-background signal ratio (henceforth called S/N) has been measured to be greater than 300 for this system.

The lock-in amplifier efficiently selects a chosen frequency from its input, (the frequency of the driving signal) and a particular phase. In this way, noise and unwanted signals are eliminated. We observe that the eddy current response of the zircaloy rods is about 60° out of phase with the UO_2 and inclusion signal and can be essentially eliminating by setting the lock-in amplifier 90° out of phase with the zircaloy signal.

At this point, we considered the application of this technique to a full-sized system. The background signal, due to the pellet-to-pellet density variation, is sure to go up because more pellets will be sampled. Also, the inclusion signal would go down because of the larger diameter pick-up coil.

The S/N for a full system is not easily estimated. We built an intermediate sized system capable of scanning a 3x3 array of 9 rods in order to test the effects of scaling up the geometry. We also wrote a computer code to predict the effect of scaling and to calculate the S/N for any size mutual inductance a.c. scanning system having the same simple coil design (see Section III).

C. An a.c. Magnetic Scanning System for a 3x3 Array

A small array of 9 rods having the geometry of an 8x8 BWR assembly was constructed of 10" zircaloy rods. We designed and built a corresponding enlarged coil system with a bore of ∿2½" (see Fig. 6).

The driving field coil (∿5Ω resistance) was driven by a power amplifier. In this case, an external signal generator provided the input signal to the amplifier as well as the reference signal to the lock-in amplifier operated in EXTERNAL mode. Again, the EMF from two bucking coils was the signal input to the lock-in amplifier.

With just 2 of the 9 zircaloy rods loaded with inclusion free (0-ppm) UO_2 pellets, the curve of Fig. 7a was obtained. If one of the center pellets was replaced with a pellet having an inclusion (∿300 ppm), the curve of Fig. 7b was produced. While the display data were taken at 20 hz, comparable results are obtained at frequencies up to several hundred hz. High frequencies provided better signal-to-noise strength due to the inductive nature of the coupling, but frequencies above an inclusion "cut-off" frequency will have reduced signal. Also, a similar response (Fig. 7c) was obtained even at a driving field strength 1/150 of the 500 gauss used in most runs.

The 66 inclusion free UO_2 pellets are not enough to fill up more than 2-10" rods. Fig. 8a,b illustrates the situation when 4 rods are partially full: the UO_2 end-effect overlaps the inclusion response. We can virtually eliminate the zircaloy end-effect (Fig. 8c) by setting the lock-in amplifier phase to be 90° out of phase with the eddy-current zircaloy signal.

With nine rods filled with 7 pellets each, the UO_2 end-effect completely overlaps the inclusion signal. A partially successful attempt was made to match the UO_2 magnetic response with strips of magnetic computer tape to reduce the end-effect (see Figure 9a,b,c). One must remember that the pervasive end-effect is an artifact of a short fuel bundle, but is not a problem in a full-sized system.

In order to compare the inclusion signal to the UO_2 background signal due to density variations in the UO_2, rods approximately 2 feet long would be required. A test using one 15" long rod run through the coil and having either no inclusions or one inclusion resulted in a S/N greater than 50. The limiting factor being the electronic noise rather than the UO_2 density variation, and the electronic noise can certainly be reduced in a more carefully constructed system (see Figure 10). Although simulating the UO_2 with other magnetically matching material could reduce the end-effect problem, it could also alter the important UO_2 background signal.

III. DATA ANALYSIS PROGRAM

A small magnetic dipole located at a height z from the plane of a circular coil will induce an EMF in that coil if the magnetic flux from the dipole linking the coil is time dependent, i.e.,

$$EMF = \oint \vec{E} \cdot d\vec{\ell} = -\frac{1}{C}\frac{d}{dt}\int_S \vec{B} \cdot \hat{n} dA. \qquad (1)$$

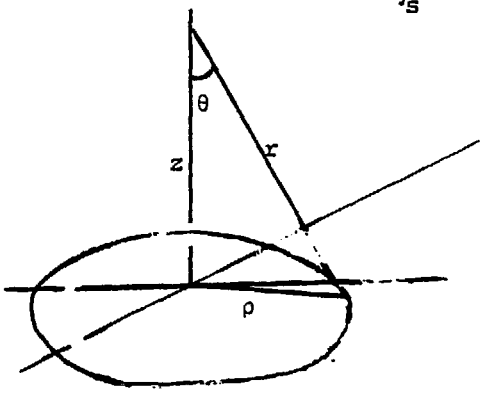

The z-component of the magnetic field of this dipole is,

$$B_z = \frac{m \cos \omega t}{r^3} (3 \cos^2\theta - 1) \qquad (2)$$

Equation (1) then becomes

$$EMF = \oint \vec{E} \cdot d\vec{\ell} = + \frac{\omega m \sin \omega t}{c} \int_0^{\rho} \left(\frac{3\cos^2\theta - 1}{r^3} \right) 2\pi\rho \, d\rho \qquad (3)$$

Since $\cos\theta = \frac{z}{r} = \frac{z}{\sqrt{z^2+\rho^2}}$ and $r^3 = {}^{3/2}\sqrt{z^2+\rho^2}$

the integral can be evaluated and the result has the form

$$EMF = \frac{2\pi m \, \omega \sin \omega t}{c} \left[\frac{1}{\sqrt{z^2+\rho^2}} - \frac{z^2}{{}^{3/2}\sqrt{z^2+\rho^2}} \right] . \qquad (4)$$

*

If instead of a point source magnetic dipole, such as an iron inclusion, we have an extended source such as a pellet, the integral becomes much more formidable. For an a.c. magnetic scanning system designed to scan many rods, the pellet radius is still much smaller than the coil radius and the point source magnetic dipole field can be used. An alternate approximation used in this program was to consider the pellet to be a linear array of point sources and the EMF then becomes the integral of the point source field over the length of the pellet; i.e., (refer to equation 4)

$$\int \frac{dz}{\sqrt{z^2+\rho^2}} = \log(z + \sqrt{z^2+\rho^2}) \qquad (6)$$

$$\int \frac{z^2 dz}{{}^{3/2}\sqrt{z^2+\rho^2}} = - \frac{z}{\sqrt{z^2+\rho^2}} + \log(z + \sqrt{z^2+\rho^2}) \qquad (6)$$

so that the difference of these two equations is simply,

---

*The bracketed term is equivalent to: $\left[\frac{(z/\rho)}{\sqrt{1+(z/\rho)^2}} \right]$

$$\frac{z}{\sqrt{z^2+\rho^2}}\Bigg|_{z}^{z+Hl} \tag{7}$$

where the limits of integration is shown and Hl is the pellet length.

The a.c. scanning system consists of two coils spaced z_o apart. If the origin of the z-axis is taken at the center of the coils, then equations (4) and (7), for the EMF for two bucking coils (BC) yields,

(for a point source)

$$(EMF)^{pt.}_{NET} = \frac{2\pi\, m\omega \sin \omega t}{c}\left[\left[\frac{1}{\sqrt{(z+z_o/2)^2+\rho^2}} - \frac{(z+z_o/2)^2}{\sqrt{(z+z_o/2)^2+\rho^2}^{3/2}}\right] - \left[\frac{1}{\sqrt{(z-z_o/2)^2+\rho^2}} - \frac{(z-z_o/2)^2}{\sqrt{(z-z_o/2)^2+\rho^2}^{3/2}}\right]\right] \tag{8}$$

and

(for an extended source)

$$(EMF)^{Pellet}_{NET} = \frac{2\pi\, m\omega \sin \omega t}{c}\left[\left[\frac{z+z_o/2+Hl}{\sqrt{(z+z_o/2+Hl)^2+\rho^2}} - \frac{z+z_o/2}{\sqrt{(z+z_o/2)^2+\rho^2}}\right] - \left[\frac{z-z_o/2+Hl}{\sqrt{(z-z_o/2+Hl)^2+\rho^2}} - \frac{z-z_o/2}{\sqrt{(z-z_o/2)^2+\rho^2}}\right]\right] \tag{9}$$

These equations were used in a computer code EMF-BC (Appendix I) to simulate the experimental results and to predict how the induced EMF would scale with changes in the coil geometric parameters.

The computer code also assumed a reasonable shape for the driving field z-dependence, i.e.,

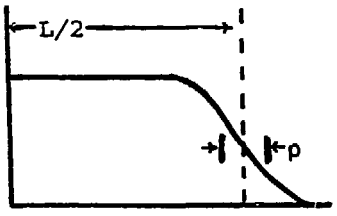

$$P_{pt.} = \frac{1}{1+be^{z/\rho}}, \tag{10}$$

where $b = e^{-L/2\rho}$

L = the length of the driving coil.

The average driving field seen by a pellet of length Hl is:

$$P^{Pellet} = \frac{\int_{z}^{z+Hl} P_{pt}\,dz}{Hl} = 1 - \frac{\rho}{Hl} \times LOG\left[\frac{1+be^{|z+Hl|/\rho}}{1+be^{|z|/\rho}}\right]. \qquad (11)$$

The EMF equations (8) and (9) should have equation (10) and (11) as z-dependent coefficients to approximate the effect of the z-dependence of the driving field.

If there are N rods and it is assumed that each rod contributes equally, the total EMF induced by N pellets located at position z becomes,

$$(EMF)_{TOT} = N_{ROD} \times (EMF)_{NET}^{Pellet} \times P^{Pellet} \qquad (12)$$

Pellets are stacked in rods and each group of N pellets at a height z contributes to the total EMF so that a sum over all pellets in the z-direction gives the final expression for the EMF. A normalization factor D_i which is proportional to the density of the N pellets at height z is included.

$$(EMF)_{TOT}^{Pellet} = \sum_{i=1}^{n} N_{ROD} \times D_i \times \left[(EMF)_{NET}^{Pellet}\right] \times P_i^{Pellet} \qquad (13)$$

Fig. 11 shows the UO_2 end-effects of a stack of 200 pellets in an 11" dia. coil system, as a function of position of the stack.

The variance of this EMF is

$$v(EMF) = N_{ROD} \times v(D_i) \times \sum_i \left[(EMF)_{NET}^{Pellet}\right]_i^2 \times \left(P_i^{Pellet}\right)^2, \qquad (14)$$

where $v(D_i)$ is the variance of the density of N_{ROD}-pellets which is a quantity easily determined.

For an inclusion of size F_e the EMF (see eqs. 8 and 10) has a typical shape shown in Fig. 11 with a maximum value called MAXY at a z-position, z_{MAX}. The ratio of the peak-to-peak signal of an iron inclusion-to-the-signal [$= v(EMF)^{\frac{1}{2}}$] of a large linear array of UO_2 pellets (S/N) is given by[9],

$$S/N = \frac{2x(MAXY)_{z_{MAX}}}{\sqrt{N_{ROD} \times v(D_i) \sum_{i=1}^{n} \left[(EMF)^{Pellet}_{NET}\right]^2_i \times \left(P_i^{Pellet}\right)^2}} \qquad (15)$$

The computer code EMF-BC calculates this quantity for each scan of a collection of rods having one inclusion in the center of a stack of n pellets high.

The results of the S/N analysis is not complete, and because of the approximations in the computer code, the validity of the results will need to be checked. Nonetheless, the results from EMF-BC are that the S/N ratio for an 8x8 BWR full-sized system (bore = 7.5" dia.) having the same relative geometry i.e., all coil dimensions scale equally, would be 13 times less than our 3x3 array; and 30 times less than our rod scanning coil geometry. The comparable numbers for a 16x16 PWR system (bore = 11" dia.) are 31 and 71.

Actual measured S/N ratios for our rod coil system are much larger than 30 (S/N measured > 300), and for the 3x3 array coil system are much larger than 13 (S/N measured > 50). By judicious choice of the coil design, the S/N ratio can be improved even further.

IV. CONCLUSIONS

A determination of the feasibility of the magnetic scanning of fresh fuel assemblies begins with an estimate of the expected S/N for a full-sized system

using the data obtained from the single rod and 3x3 array system constructed at BNL. (Fig. 12). These data will require corroboration and where deficient, will have to be repeated. The analysis program used in the scaling-up to a full-sized system will also require verification and again where better approximations in the analysis are needed, they will have to be included. To the extent that the S/N values measured to date are accurate and the approximations used in BNL's program EMF-BC are acceptable, the scaling up analysis indicates sufficient S/N to warrent construction of a full-sized system to scan either BWR or PWR fresh fuel assemblies based on an a.c. magnetic system. Better S/N results can probably be obtained with more sophisticated coil design.

Before a system is designed for scanning spent fuel assemblies, some questions have to be addressed, such as:

a) Signature changes:

- What happens to an inclusion after 3 years exposure in a reactor core? If the inclusion is Fe_3O_4, probably not much of a change.[10]
- What additional magnetic materials appear in or on an assembly after it comes out of the core and into the SFSP? Here the concern is mainly magnetic "crud" that can cling to the assemblies.
- If the signature changes, can a new magnetic signature be obtained and used for the remainder of the assemblies' life?

b) How diversion deterrent is a magnetic signature of an assembly and how can the scanning system be designed to increase the deterrance? Perhaps a simultaneous axial and transverse field scan (x-y-z information) that is sensitive to inclusion orientation is feasible.

c) How best can the spent fuel assemblies be scanned underwater with the constraint of minimum movement of assemblies?

d) What is the projected cost of both a spent fuel scanning system and a

fresh fuel system? (A fresh fuel system would probably cost only $10-20K).

At this early stage in the development of a new LWR fuel identification system, most of these questions seem premature. Reference 1 points out that the development of a fast and secure fuel identification system for fresh fuel alone - either UO_2 or mixed-oxide-could aid the Agency considerably in meeting its safeguard requirements. Finally, the lack of other fully acceptable methods for identifying fresh or spent fuel assemblies should mitigate against placing too great a burden on a new promising system before proceding with modest development.

ACKNOWLEDGEMENT

This work could not have been attempted without the cheerful cooperation of Jim Hurst of BNL's physics department. We like to thank Marty Zucker who provided the rod coil and Frank Merkert of BNL who wound the large coils for the 3x3 array. The full cooperation of Dr. Fred Schoenig of G.E., Wilmington in providing pellets on loan and helpful advice all during this program was invaluable.

REFERENCES

1. Letter from A. von Baeckmann to G. Weisz, 2/5/80.

2. McKenzie, J.M. et al., "Current Status of a Fuel Assembly Identification Device for BWR Fuel Assemblies," and "A System to Establish the Inherent Identity of Westinghouse PWR Fuel Assemblies," 2nd Annual Symposium on Safeguards and Nuclear Material Management, ESARDA, Edinburgh, Scotland, March 26-28, 1980, pp. 455, 458.

3. Fiarman, S., "Systems for Sealing LWR Fuel Assemblies," ISPO-75, October, 1978.

4. Surasky, A.A., "Magnetic and Passive Scanners (MAPS) - Overview", G.E. Report NEDO-21979/78NED161, October, 1978.

5. Schoenig, F.C., "Magnetic Tamper Safing of Nuclear Fuel Bundles", unpublished, 1978.

6. Foner, S., "Versatile and Sensitive Vibrating-Sample Magnetometer," The Review of Scientific Instruments 30 (1959) 548.

7. Handbook of Physics and Chemistry, CRC Press, 55th Edition, p. E-125.

8. P. Swartz, Intermagnetics General Corporation, private communications, 1980.

9. Jon Sanborn, BNL/TSO, private communication, 1980.

10. Tom Lukman, BNL, private communication, 1979.

FIGURE CAPTIONS

Figure 1 Magnetization curves for a) pellet with no inclusion, b) pellet with an inclusion, and c) an iron particle.

Figure 2 Specifications for a rod coil assembly.

Figure 3 Schematic diagram of the rod scanning system's electronics.

Figure 4 Time response of 6 pellets passing through the rod scanning system.

Figure 5 Time response of 6-0 ppm pellets and 1 ~600 ppm inclusion pellet passing through the rod scanning system.

Figure 6 Specifications for the 3x3 array, the driver coil assembly and the pick-up coil assembly.

Figure 7 Two rods of 3x3 array filled with a) 0-ppm UO_2 pellets, b) one 0-ppm pellet replaced by a 500 ppm pellet. Figure 7c same as 7b but with driver field reduced by factor of 150.

Figure 8 Four rods of 3x3 array filled with a) 0-ppm UO_2 pellets, b) one 0-ppm pellet replaced by a 500 ppm pellet. Figure 8c indicates position of zircaloy end-effect in this geometry.

Figure 9 Nine rods of 3x3 array filled with 7 pellets each having a) only 0-ppm UO_2 pellets, b) one 0-ppm pellet replaced by a 500 ppm pellet. Figure 9c shows the typical inclusion response when curve (a) is subtracted from curve (b).

Figure 10 A 15" rod in 3x3 array with a) no inclusions and b) one 0-ppm pellet replaced by a 500 ppm pellet.

Figure 11 Computer output from EMF-BC showing UO_2 end-effects and inclusion effect. The program input parameters are shown along with the results of the S/N calculation.

Figure 12 Photograph of the BNL single rod and 3x3 array system.

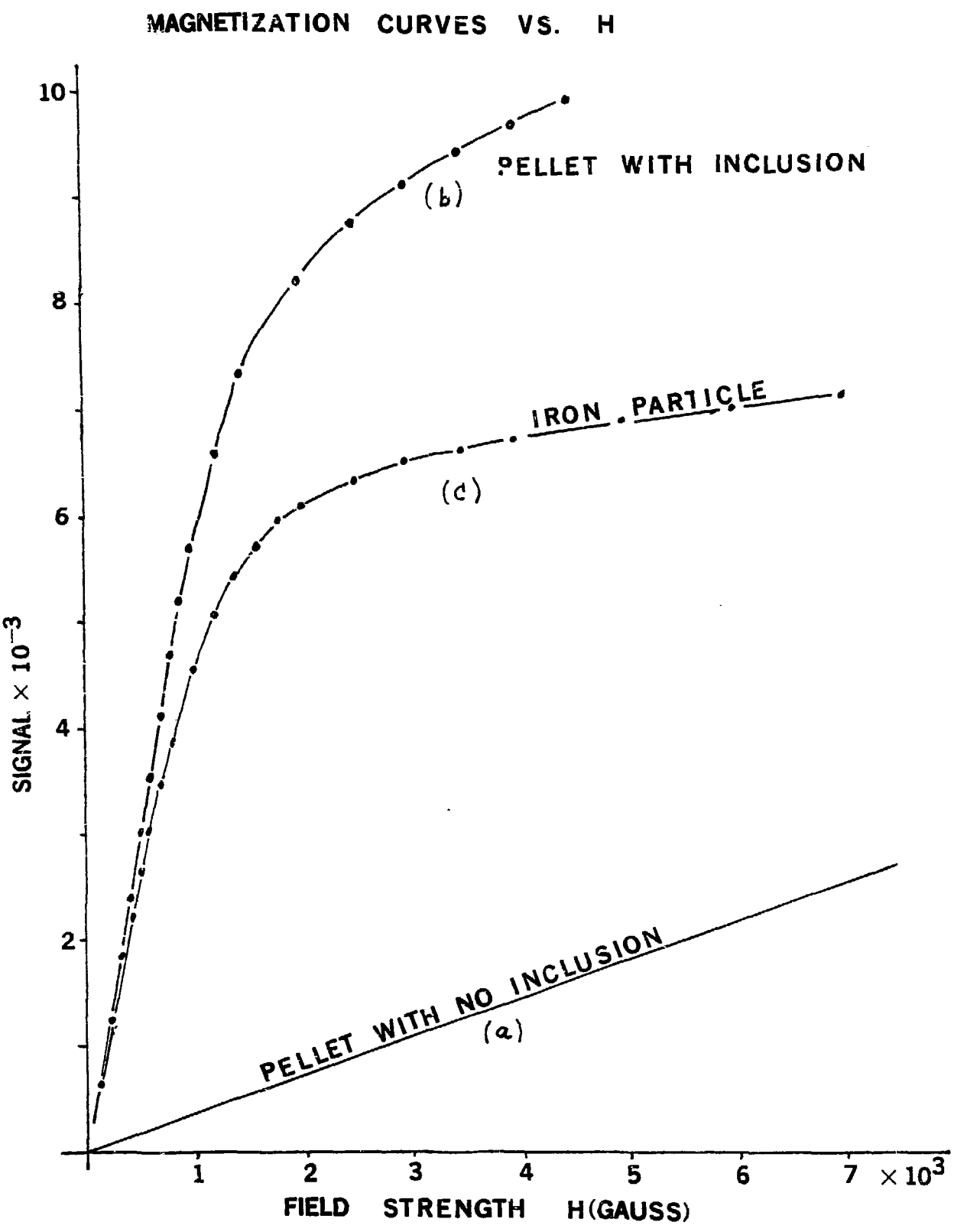

Figure 1 Magnetization curves for a) pellet with no inclusion, b) pellet with an inclusion, and c) an iron particle.

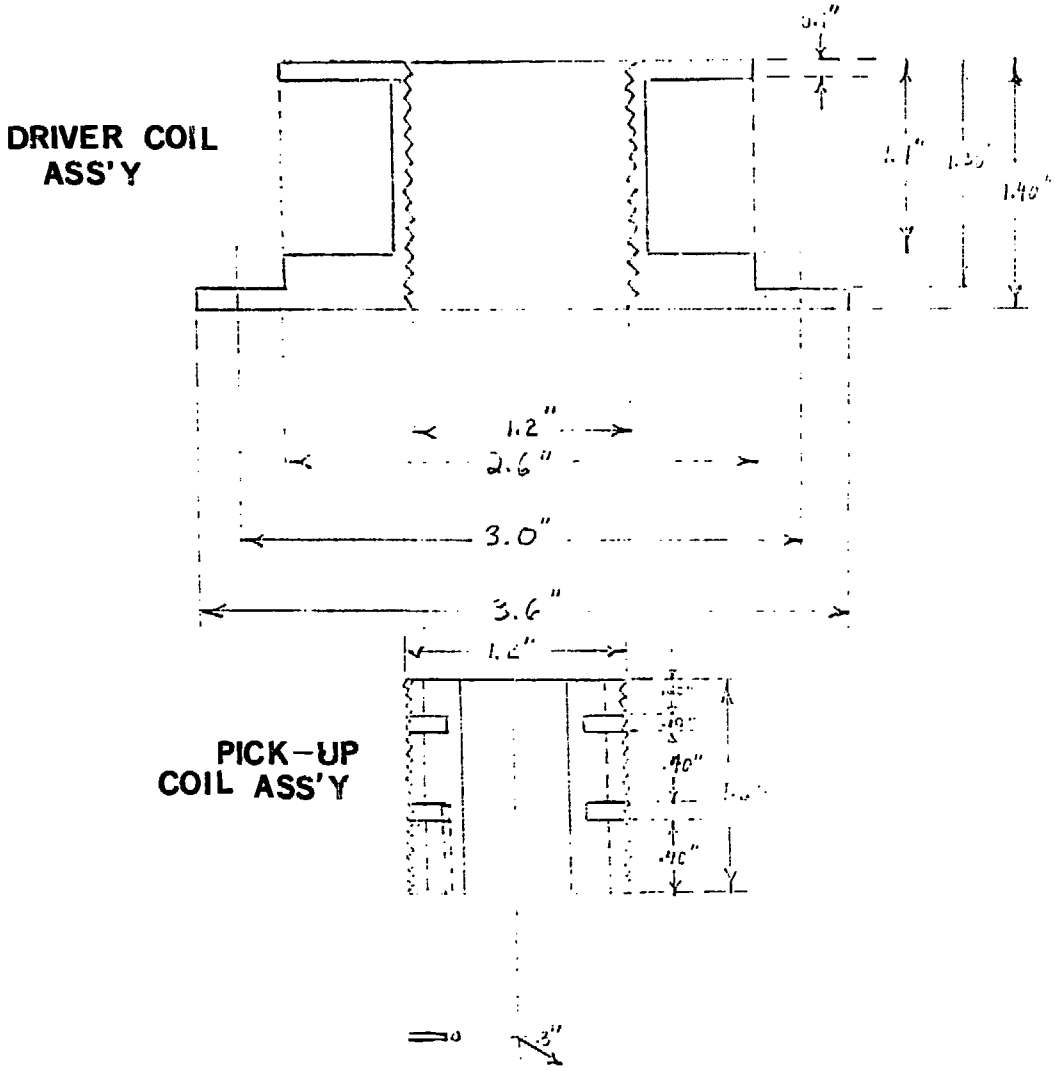

Figure 2 Specifications for a rod coil assembly.

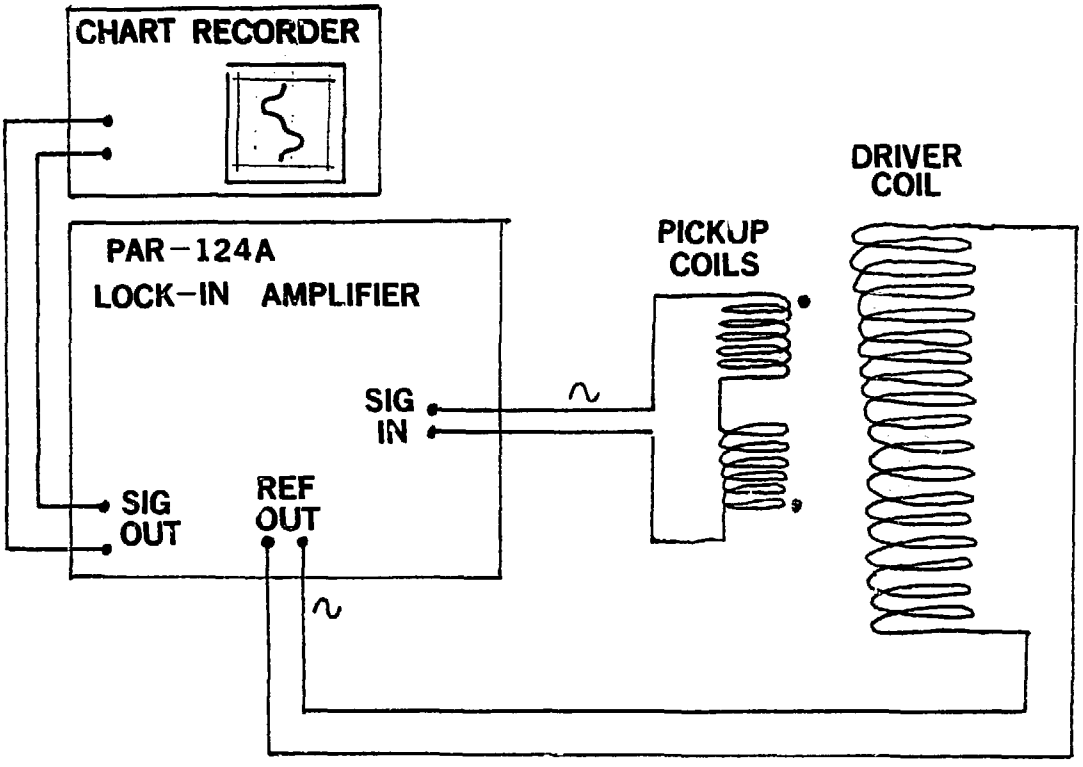

Figure 3 Schematic diagram of the rod scanning system's electronics.

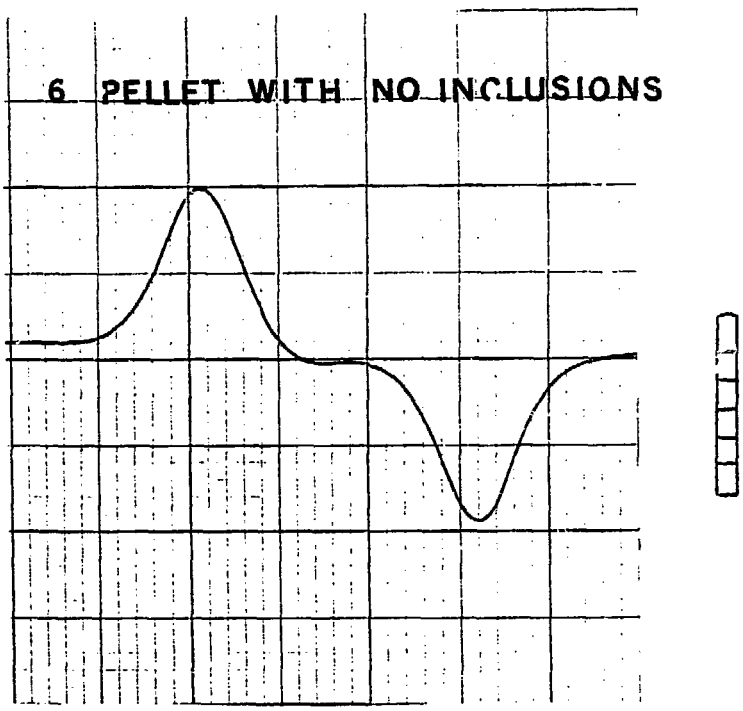

Figure 4 Time response of 6 pellets passing through the rod scanning system.

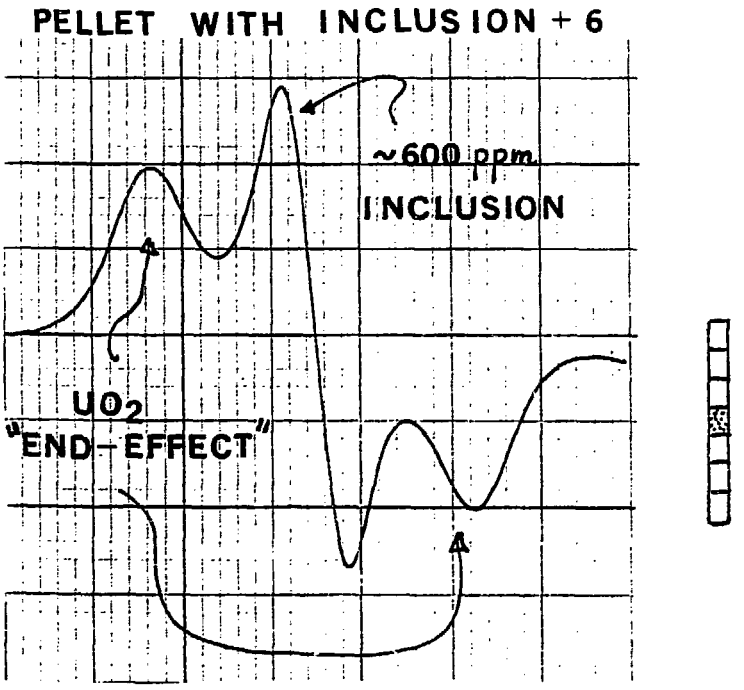

Figure 5 Time response of 6-0 ppm pellets and 1 ~600 ppm inclusion pellet passing through the rod scanning system.

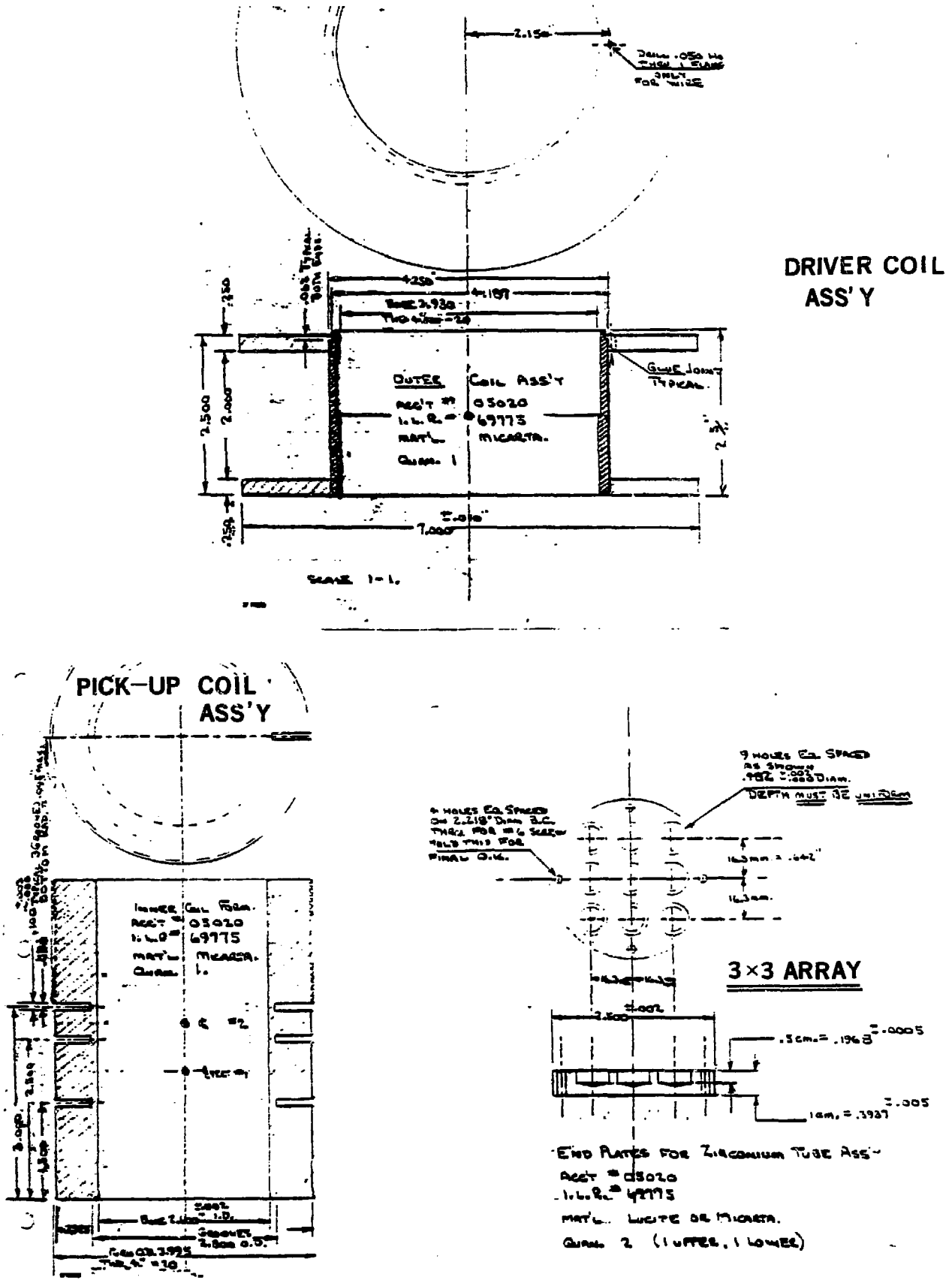

Figure 6 Specifications for the 3x3 array, the driver coil assembly and the pick-up coil assembly.

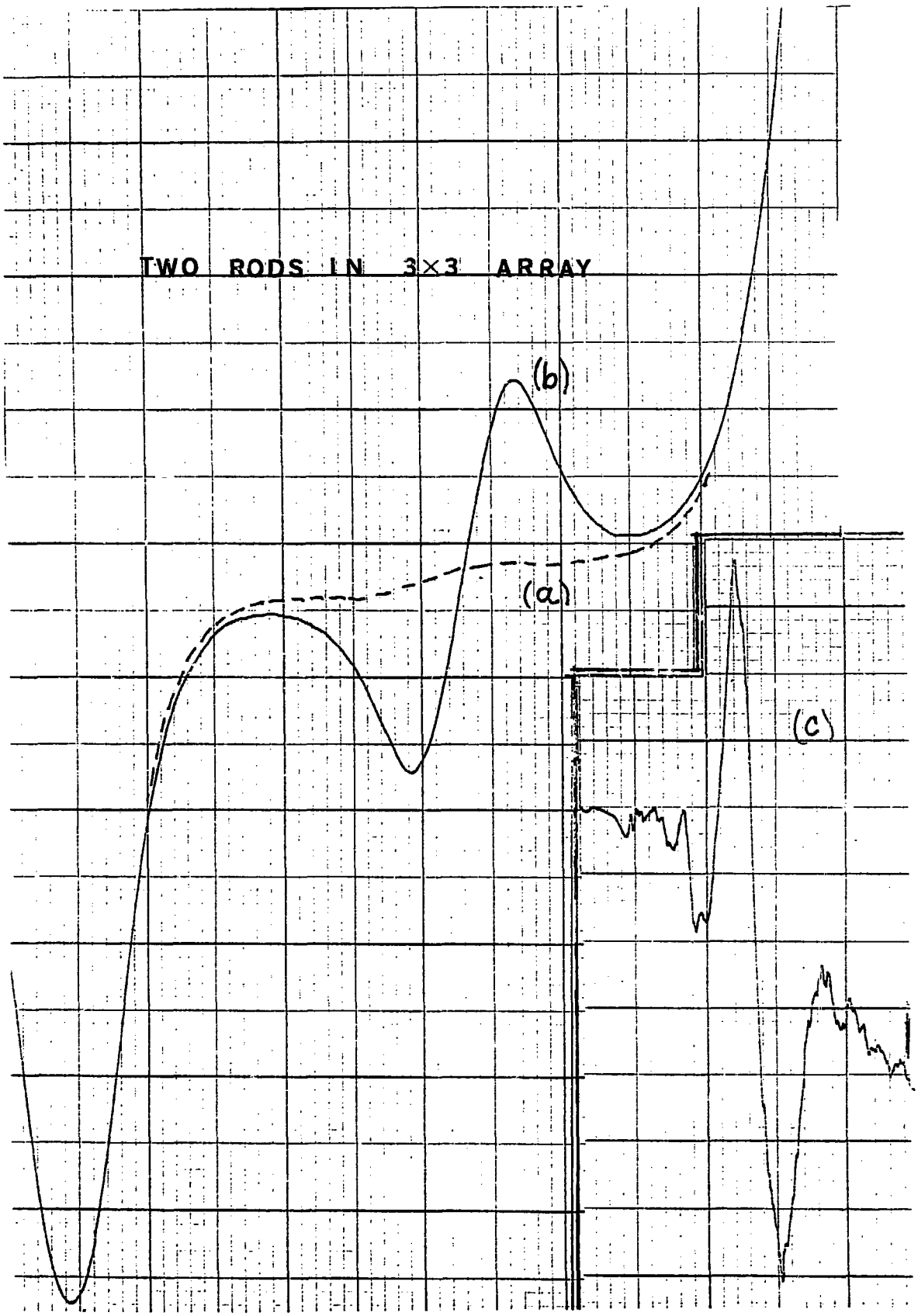

Figure 7 Two rods of 3x3 array filled with a) 0-ppm UO_2 pellets, b) one 0-ppm pellet replaced by a 500 ppm pellet. Figure 7c same as 7b but with driver field reduced by factor of 150.

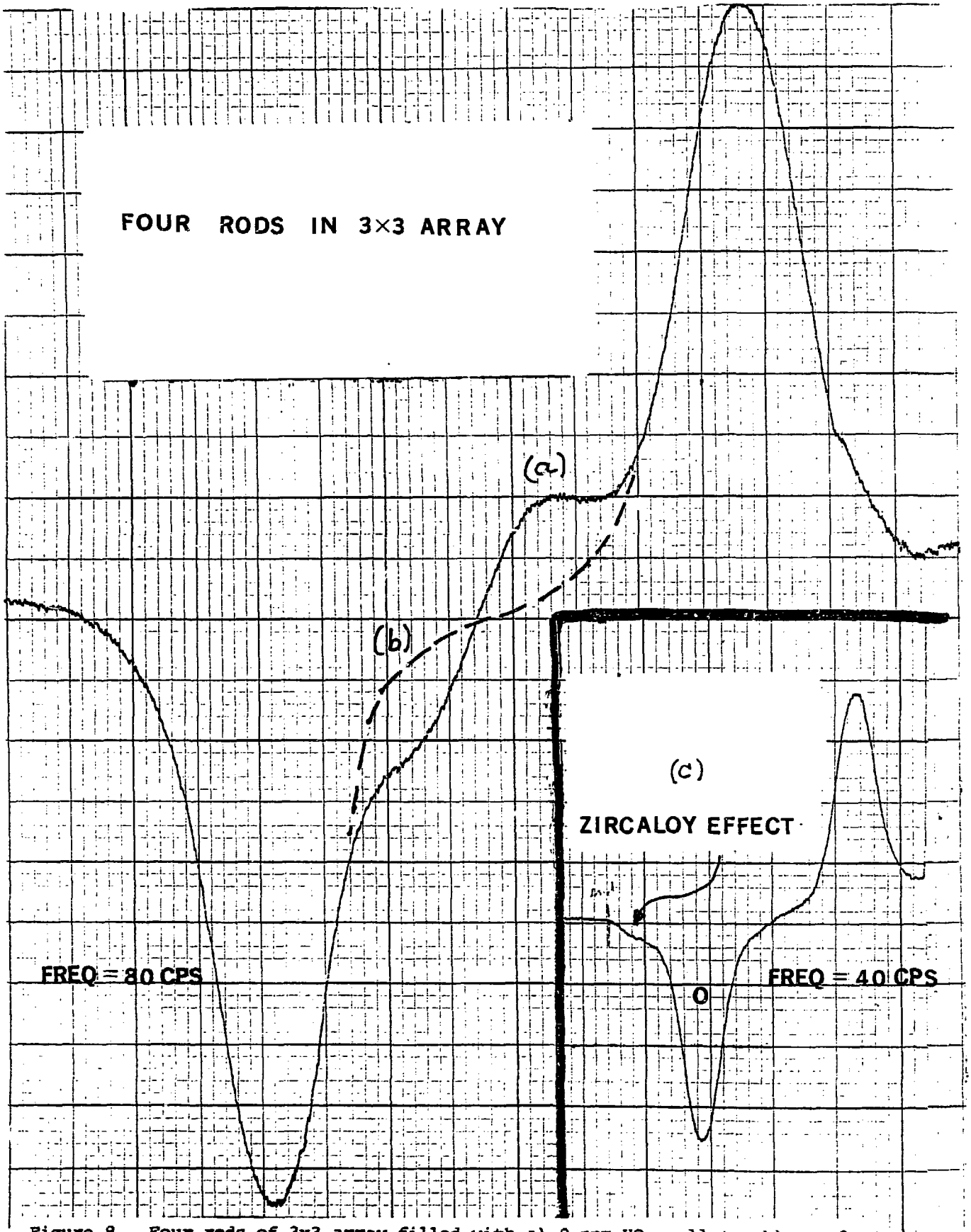

Figure 8 Four rods of 3x3 array filled with a) 0-ppm UO_2 pellets, b) one 0-ppm pellet replaced by a 500 ppm pellet. Figure 8c indicates position of zircaloy end-effect in this geometry.

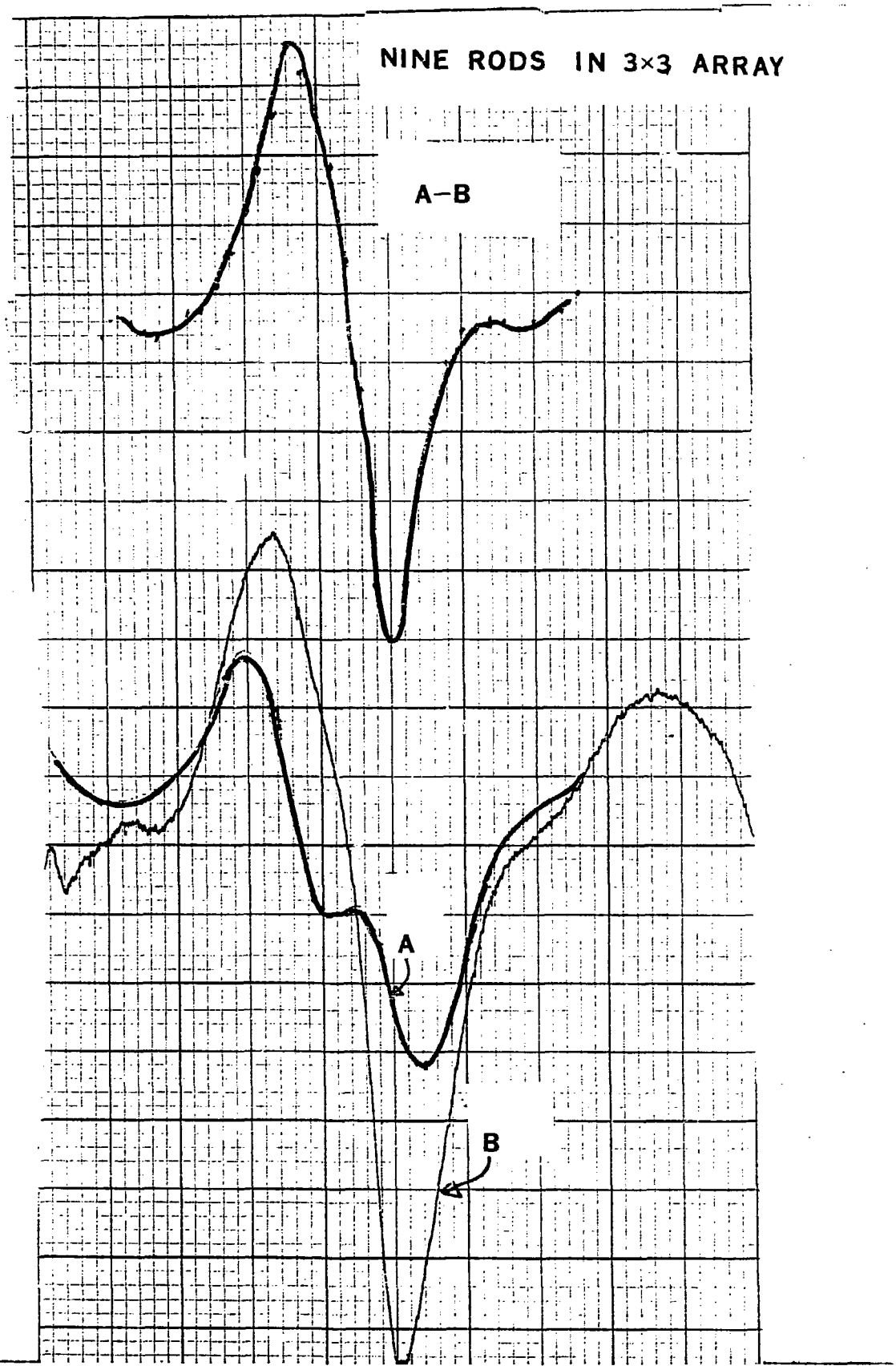

Figure 9 Nine rods of 3x3 array filled with 7 pellets each having a) only 0-ppm UO_2 pellets, b) one 0-ppm pellet replaced by a 500 ppm pellet. Figure 9c shows the typical inclusion response when curve (a) is subtracted from curve (b).

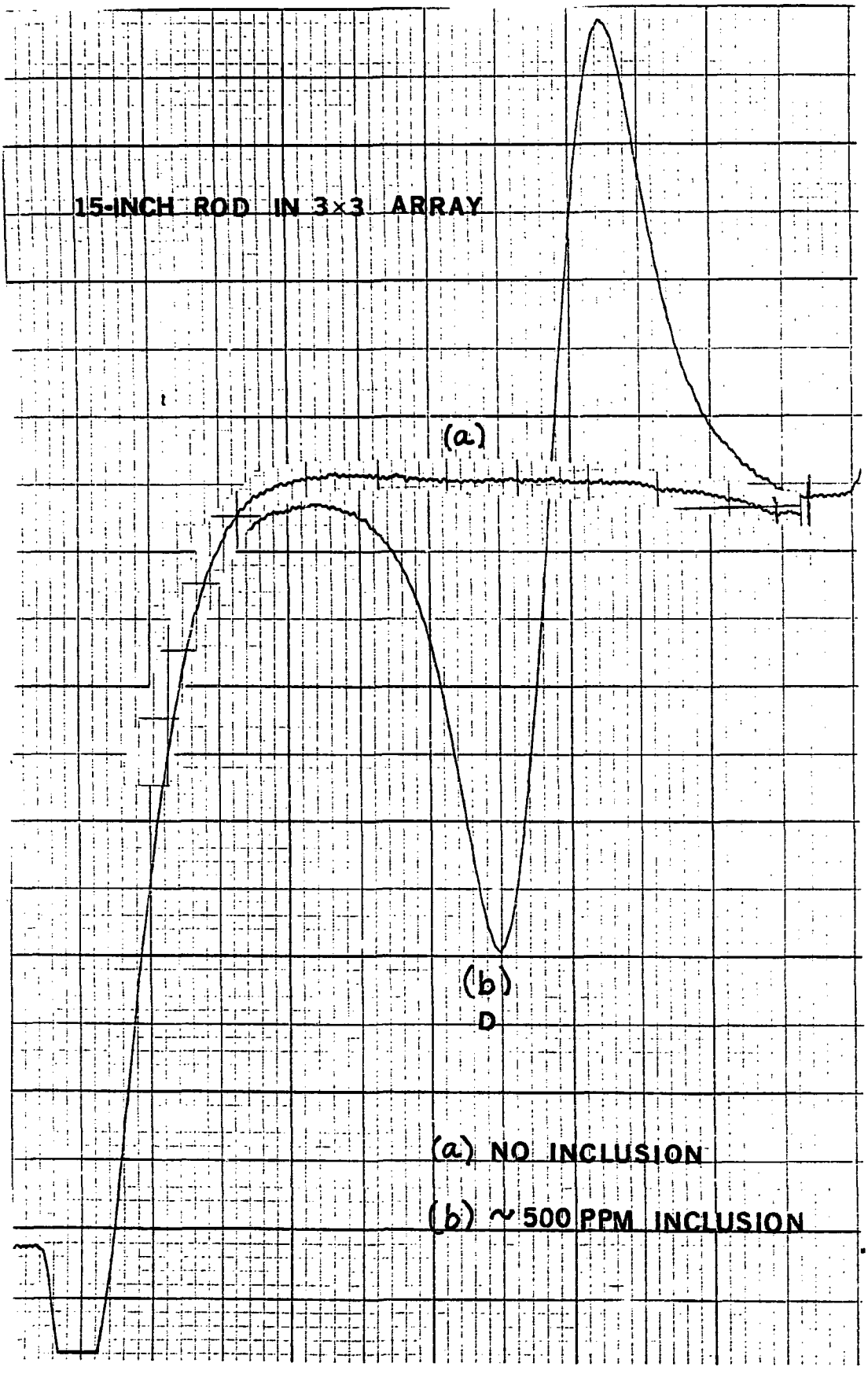

Figure 10 A 15" rod in 3x3 array with a) no inclusions and b) one 0-ppm pellet replaced by a 500 ppm pellet.

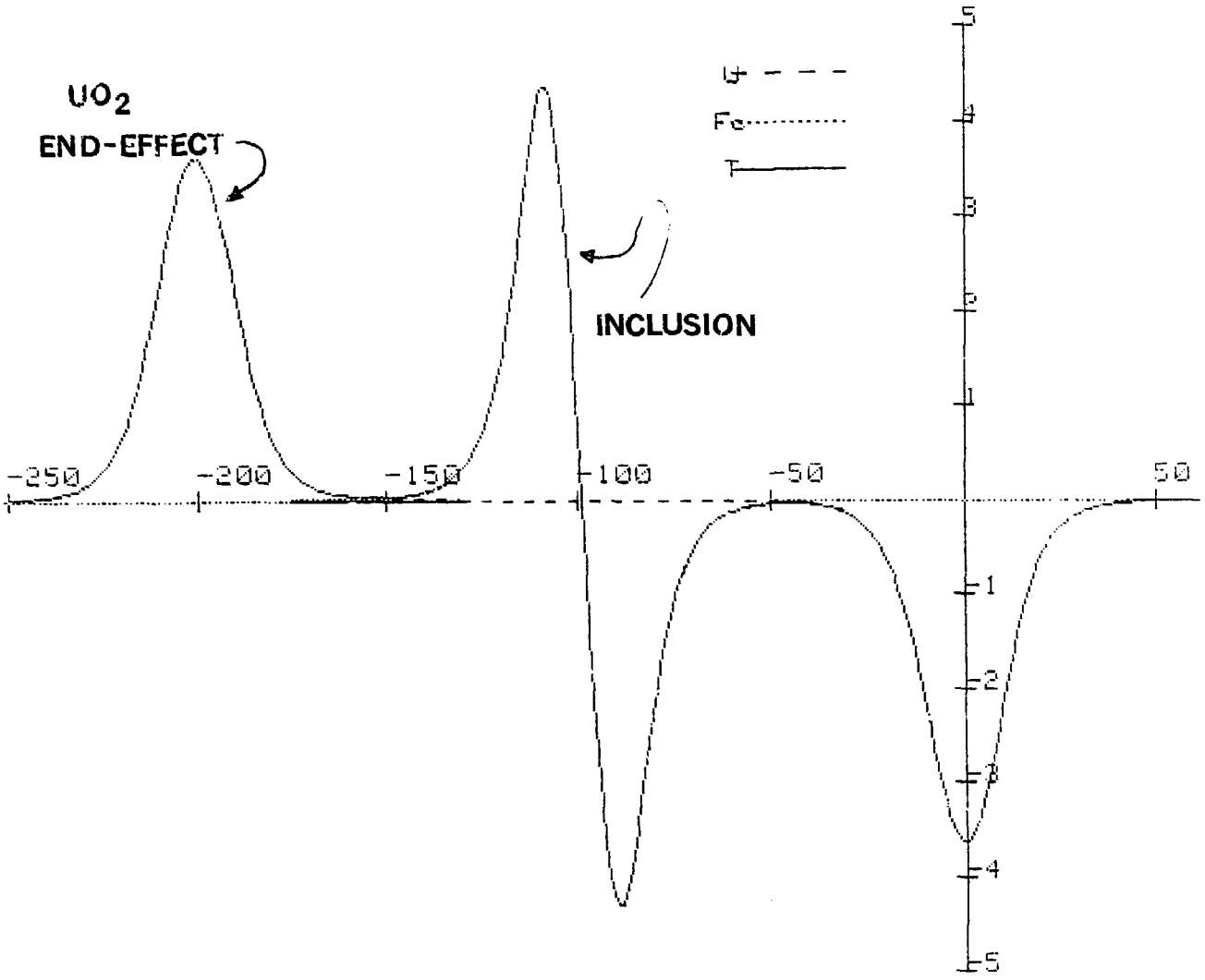

Radius= 13.97 Coil spacing= 17.46 Pellet size= 1 No. of Pellets= 200

Starting height= 60 Ending height=-250 Step size= 1

UU2= 5 Fe= 100 RUN #= 3 S/N= .862372232793

Driver coil length= 55.88 Density Fluctuation (0-1)= 0

Variance= .1 Nrod= 235 Nfe= 100

Figure 11 Computer output from EMF-BC showing UO_2 end-effects and inclusion effect. The program input parameters are shown along with the results of the S/N calculation.

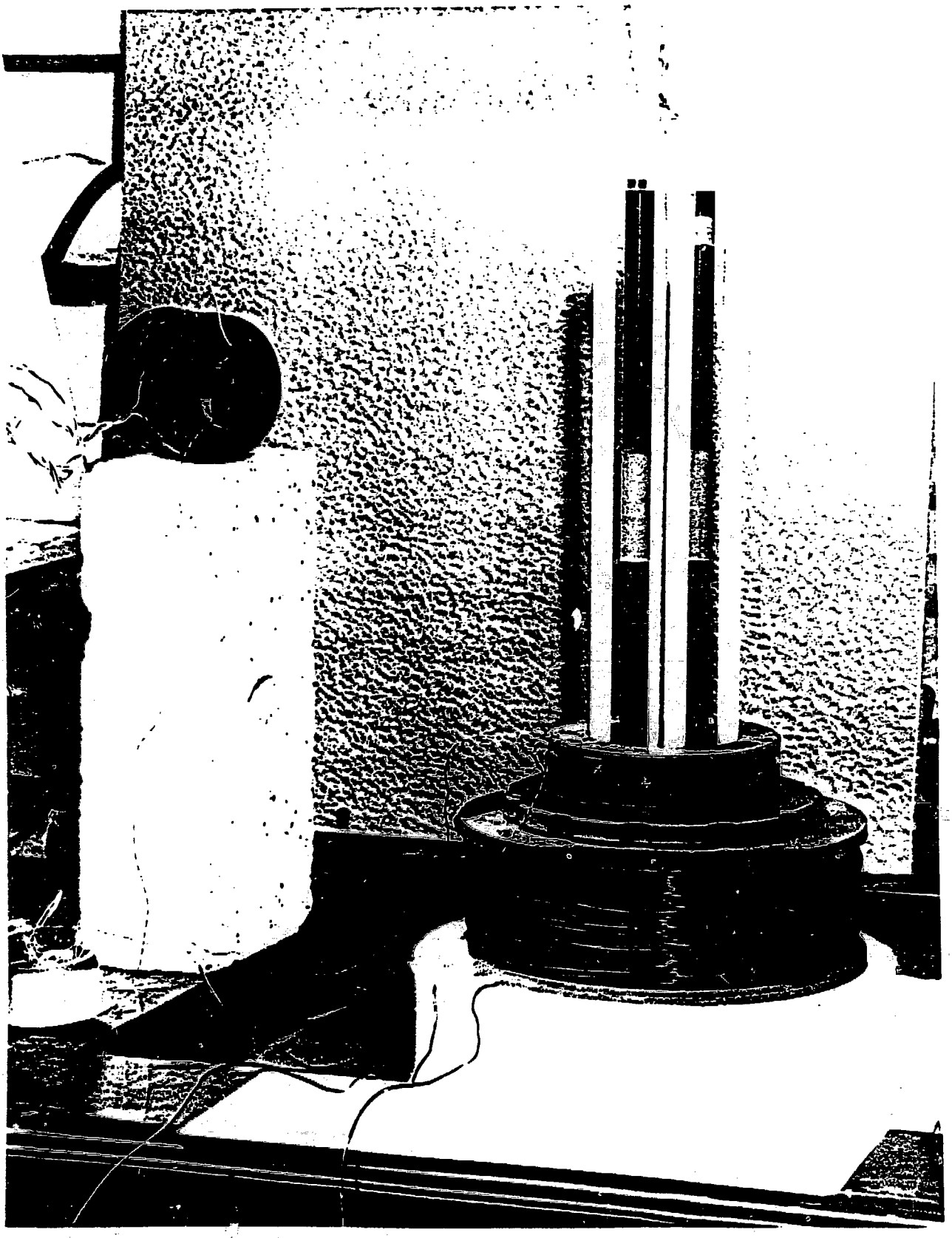

Figure 12 Photograph of the BNL single rod and 3x3 array system.

APPENDIX I

Computer Program EMF-BC

```
10     REM ************** "EMF-BC" ********************8/10/90
20     DIM Efe(300),Etotal(300),H(300),Ffe(300),Uuo2(300),Hfe(300)
30     DIM Uuo3(300),Euo1(300),Euo2(300),Euo3(300),Rd(300)
40   ! FOR TWO BUCKING COILS OF RADIUS R AND SPACING H0 IN AN AC DRIVING
50   ! FIELD GENERATED BY A COIL OF LENGTH L
131    OUTPUT 9;"R"
132    ENTER 9;Month,Day,Hour,Minute,Sec
133    RANDOMIZE Sec/(Day*Hour*Minute)
140    INPUT "RADIUS?",R
150    INPUT "COIL SPACING?",H00
160    INPUT "PELLET SIZE?",H1
170    INPUT "NUMBER OF PELLETS?",Np
180    INPUT "DENSITY FLUCTUATIONS (0-1),VARIANCE?",F,Var
190    INPUT "INCLUSION PELLET NUMBER?",Nfe
200    INPUT "STARTING HEIGHT?",Hs
210    INPUT "ENDING HEIGHT?",He
220    INPUT "STEP SIZE?",Ssize
230    INPUT "UO2,FE?",Uo2,Fe
240    INPUT "DRIVER COIL LENGTH ?",L
241    INPUT "NUMBER OF RODS?",Nrod
250    H0=H00/2
270    MAT Euo1=ZER
271    MAT Euo2=ZER
272    MAT Euo3=ZER
280    Maxy=0
290    I=2*Hs/Ssize
300    Cos=L/2/SQR((L/2)^2+R^2)
310    J=0
311  ! Start moving pellets down _ stepping with J
320    J=J+1
321  ! Locate Position of first pellet
322    H(J)=Hs-Ssize*(J-1)
330    N=0
331  ! Start sum over pellets
340    N=N+1
341    IF J>1 THEN 350
342    Rd(N)=RND
350    IF N>No THEN 560
361  ! Locate Fe inclusion
370    Hfe(J)=Hs+H1*(N-1/2)-Ssize*(J-1)
380    A=(H(J)+(N-1)*H1-H0)/R
390    B=(H(J)+N*H1-H0)/R
400    Ap=(H(J)+(N-1)*H1+H0)/R
410    Bp=(H(J)+N*H1+H0)/R
420    Bb=EXP(-L/(2*R))
430    U=R/H1
431  ! Calculate driving field coefficient
440    Z=1-U*ABS(LOG((1+Bb*EXP(ABS(H(J)+N*H1)/R))/(1+Bb*EXP(ABS(H(J)+(N-1)*H1)/R)
)))
460    IF SGN(H(J)+N*H1)=SGN(H(J)+(N-1)*H1) THEN 471
461    Z=1-U*ABS(LOG((1+Bb)/(1+Bb*EXP(ABS(H(J)+(N-1)*H1)/R))))-U*ABS(LOG((1+Bb)/(
1+Bb*EXP(ABS(H(J)+N*H1)/R))))
462  ! Calculate coefficient for emf including random density fluctuation
471    Uuo2(J)=Uo2*(1+F*Rd(N))*Z
472    Y=H(J)+(N-1)*H1
473    Y1=Y+H0
474    Y2=Y-H0
475    Y1p=Y1+H1
476    Y2p=Y2+H1
477    Coil1=Y1p/SQR(Y1p^2+R^2)-Y1/SQR(Y1^2+R^2)
478    Coil2=Y2p/SQR(Y2p^2+R^2)-Y2/SQR(Y2^2+R^2)
490    Euo2(J)=(Coil1-Coil2)*Uuo2(J)
491    Euo1(J)=Euo2(J)+Euo1(J)
492    Euo3(J)=Euo2(J)^2+Euo3(J)
493  ! Is this the pellet with the iron inclusion?
```

```
500   IF N=Nfe THEN 511
501   GOTO 340
502 ! Fe inclusion calculation
511   Ffe(J)=Fe/(1+Bb*EXP(ABS(Hfe(J))/R))
512   Koil1=1/SQR(Y1^2+R^2)-Y1^2*(Y1^2+R^2)^(-1.5)
513   Koil2=1/SQR(Y2^2+R^2)-Y2^2*(Y2^2+R^2)^(-1.5)
514   Efe(J)=Ffe(J)*(Koil1-Koil2)
550   GOTO 340
560   Etotal(J)=Euo1(J)+Efe(J)
570   Maxy1=ABS(Etotal(J))
580   IF Maxy<=Maxy1 THEN Maxy=Maxy1
590   DISP J,Maxy,RND
600   IF H(J)=He THEN 620
610   GOTO 320
620   PRINTER IS 0
621   Sig=Euo3(J/2)
622   Bton=Maxy/SQR(Nrod*Var*Sig)
630   I=J
640   BEEP
650   INPUT "DO YOU WANT A PRINTOUT?",Ans$
660   IF Ans$="NO" THEN 740
670   IMAGE 2X,A,5(9X,6A )
680   PRINT USING 670;"H","EUO1","EFe","ETotal","Bfe","Buo2"
690   IMAGE MDD.DD,2X,4(MDD.DDDDD,6X), MDDD.DDDD
700   FOR J=1 TO I
710   PRINT USING 690;H(J),Euo1(J),Efe(J),Etotal(J),Ffe(J),Uuo2(J)
720   NEXT J
730   PRINT PAGE
740   PLOTTER IS 13,"GRAPHICS"
750   GRAPHICS
760   LOCATE 0,122,0,98
770   SCALE INT(He)-1,INT(H(1)+1),-INT(Maxy)-1,INT(Maxy)+1
780   AXES 1,1,0,0
790   LORG 1
800   FOR K=INT(He)-1 TO INT(H(1))+1
810   IF K=0 THEN 840
820   MOVE K,.2
830   LABEL USING "K";K
840   NEXT K
850   FOR K=-INT(Maxy)-1 TO INT(Maxy)+1
860   IF K=0 THEN 890
870   MOVE .2,K
880   LABEL USING "K";K
890   NEXT K
900   LORG 5
910   CSIZE 3
920   LINE TYPE 4,2
930   FOR J=1 TO I
940    IF J=1 THEN MOVE H(J),Euo1(J)
950                DRAW H(J),Euo1(J)
960   NEXT J
970   LINE TYPE 3
980   FOR J=1 TO I
990   IF J=1 THEN MOVE H(J),Efe(J)
1000  DRAW H(J),Efe(J)
1010  NEXT J
1020  LINE TYPE 1
1030  FOR J=1 TO I
1040  IF J=1 THEN MOVE H(J),Etotal(J)
1050  DRAW H(J),Etotal(J)
1060  NEXT J
1070  LINE TYPE 1
1080  MOVE INT(-He),(INT(Maxy)+1)*.9
1090  LABEL USING "K";"U"
1100  MOVE INT(-He)+.2,(INT(Maxy)+1)*.9
1110  LINE TYPE 4,2
```

```
1120  DRAW INT(-Hs)/2,(INT(Maxy)+1)*.9
1130  MOVE INT(-Hs),(INT(Maxy)+1)*.8
1140  LINE TYPE 1
1150  LABEL USING "K";"Fe"
1160  MOVE INT(-Hs)+.2,(INT(Maxy)+1)*.8
1170  LINE TYPE 3
1180  DRAW INT(-Hs)/2,(INT(Maxy)+1)*.8
1190  LINE TYPE 1
1200  MOVE INT(-Hs),(INT(Maxy)+1)*.7
1210  LABEL USING "K";"T"
1220  MOVE INT(-Hs)+.2,(INT(Maxy)+1)*.7
1230  DRAW INT(-Hs)/2,(INT(Maxy)+1)*.7
1240  PAUSE
1250  INPUT "DO YOU WANT A HARD COPY?",Ans$
1260  IF Ans$="NO" THEN 1331
1270  DUMP GRAPHICS
1280  EXIT GRAPHICS
1290  PRINT LIN(3),"Radius=";R,"Coil spacing=";2*H0,"Pellet size=";H1,"No. of Pe
llets=";Np,LIN(1)
1300  PRINT "Starting height=";Hs,"Ending height=";He,"Step size=";Ssize,LIN(1)
1310  PRINT "UO2=";Uo2,"Fe=";Fe,"      RUN #=";3-Rr,"S/N=";Ston,LIN(1)
1320  PRINT "Driver coil length=";L,"Density Fluctuation (0-1)=";F,"Variance=";V
ar,"Nrod=";Nrod,"Nfe=";Nfe,LIN(1)
1330  PRINT PAGE
1331  EXIT GRAPHICS
1340  GOTO 140
1350  STOP
1360  END
```